Title

Hippocampal Connectivity with the Default Mode Network is Linked to Hippocampal Volume in the Clinical High Risk for Psychosis Syndrome and Healthy Individuals.

Permalink

Journal

ISSN

Authors

Aberizk, Katrina

Sefik, Esra

Addington, Jean

et al.

Publication Date

DOI

Peer reviewed

Hippocampal Connectivity with the Default Mode Network is Linked to Hippocampal Volume in the Clinical High Risk for Psychosis Syndrome and Healthy Individuals

Katrina Aberizk[a], Esra Sefik[a,b], Jean Addington[c], Alan Anticevic[d], Carrie E. Bearden[e], Kristin S. Cadenhead[f], Tyrone D. Cannon[d], Barbara A. Cornblatt[g], Matcheri Keshavan[h], Daniel H. Mathalon[i,j], Diana O. Perkins[k], William S. Stone[h], Ming T. Tsuang[f], Scott W. Woods[d], Elaine F. Walker[a]

[a]Department of Psychology, Emory University, Atlanta, GA, USA

[b]Department of Human Genetics, Emory University School of Medicine, Atlanta, GA, USA

[c]Department of Psychiatry, University of Calgary, Calgary, AB, Canada

[d]Department of Psychiatry, Yale University, New Haven, CT, USA

[e]Semel Institute for Neuroscience and Human Behavior, Departments of Psychiatry and Biobehavioral Sciences and Psychology, University of California, Los Angeles, CA, USA

[f]Department of Psychiatry, University of California, San Diego, CA, USA

[g]Department of Psychiatry, Zucker Hillside Hospital, New York City, NY, USA

[h]Department of Psychiatry, Harvard Medical School, Harvard University, Cambridge, MA, USA

[i]Department of Psychiatry, University of California, San Francisco, CA, USA

[j]San Francisco VA Medical Center, San Francisco, CA, USA

[k]Department of Psychiatry, University of North Carolina, Chapel Hill, NC, USA

Abstract

Reduced hippocampal volume (HV) is an established brain morphological feature of psychiatric conditions. HV is associated with brain connectivity in humans and non-human animals and altered connectivity is associated with risk for psychiatric illness. Associations between HV and connectivity remain poorly characterized in humans, and especially in phases of psychiatric illness that precede disease onset. This study examined associations between HV and hippocampal functional connectivity (FC) during rest in 141 healthy controls and 248 individuals at-risk for

psychosis. Significant inverse associations between HV and hippocampal FC with the inferior parietal lobe (IPL) and thalamus were observed. Select associations between hippocampal FC and HV were moderated by diagnostic group. Significant moderation results shifted from implicating the IPL to the temporal pole after excluding participants on antipsychotic medication. Considered together, this work implicates hippocampal FC with the temporoparietal junction, within a specialized subsystem of the default mode network, as sensitive to HV.

Introduction

The hippocampus has been the focus of considerable attention in research on psychiatric disorders. Reduced hippocampal volume (HV) is the most established brain morphological feature of several psychiatric conditions, including psychosis (van Erp et al., 2015). In contrast, meta-analyses have concluded that there are no significant baseline differences in bilateral HV between individuals at clinical high-risk for psychosis (CHR-P) and comparison subjects (Walter et al., 2016) or between individuals at CHR-P who develop psychosis and those who do not (Hinney et al., 2021). Taken together, these findings suggest that reductions in HV occur proximal to the clinical onset of psychosis in those who develop psychotic disorders.

A growing body of literature suggests that reductions in HV are associated with aberrant hippocampal activity in humans with psychiatric illness. Early evidence for this association was found in post-mortem studies of individuals with chronic schizophrenia (SZ), the most severe psychotic disorder, which demonstrated that a selective loss of GABAergic interneurons is the primary contributor to reductions in HV in those who develop psychosis (Benes & Berretta, 2001). Mice genetically engineered to model the loss of a significant risk gene implicated in SZ have also demonstrated hippocampal degeneration involving significant losses of GABAergic interneurons (Dickerson et al., 2002). Inhibitory GABAergic neurotransmission synchronizes the firing of excitatory pyramidal cell populations (Cauli et al., 2004). This coordinated neural activity is required to efficiently shunt oxygenated blood through the brain, a process known as neurovascular coupling, which yields the normative expression of blood-oxygenation-level-dependent (BOLD) signals that are detected during functional magnetic resonance imaging (fMRI) (Cabral et al., 2011; Lecrux et al., 2011; Logothetis & Pfeuffer, 2004). Prolonged BOLD signal putatively indicates the maintenance of neural responses (Hillman, 2014), and BOLD signal forms the unit of analysis when modeling functional connectivity (FC) (Lecrux et al., 2011). FC indexes covariation in BOLD signal, and brain regions maintain FC if BOLD signal at one region covaries with signal at another region (Mevel et al., 2011).

Declines in GABAergic neurotransmission putatively bias the hippocampus toward a hyperactive state that requires increased blood flow to maintain (Heckers & Konradi, 2015). Increased cerebral blood flow to the hippocampus is a well-replicated finding in individuals at CHR-P (Modinos et al., 2021; Schobel et al., 2013), which suggests that the hippocampus is hyperactive during the prodrome to psychoses (Provenzano et al., 2020). Findings demonstrating heightened hippocampal activity (Modinos et al., 2021; Provenzano et al., 2020; Schobel et al., 2013) in prodromal psychoses, coupled with evidence that these

aberrations may, in part, reflect progressive losses of inhibitory cells (Benes & Berretta, 2001), suggests that hippocampal connectivity may be associated with HV.

The hippocampus carries a higher communication load than many other brain regions and serves as a hub of the default mode network (DMN) (Bassett & Sporns, 2017), which has been described as the apex transmodal network responsible for coordinating integrative cognitive processes (Buckner & DiNicola, 2019). This hierarchical organization of brain regions and networks is thought to support efficient neurotransmission, yet aberrations to the function or structure of hub regions may dramatically affect neurotransmission within and between networks involving the implicated region (Gong et al., 2009). Consistent with that notion, prior work demonstrated progressive declines in brain network modularity, or functional segregation, as measured with fMRI, in individuals at CHR-P who developed psychosis. More specifically, those global declines in brain network modularity were driven by increases in path length within the DMN, which suggests that functional aberrations in the DMN drive global inefficiencies in neurotransmission as psychosis develops (Cao et al., 2020).

A limited number of published studies on relationships between HV and connectivity in individuals with SZ and their first-degree relatives have indeed demonstrated that HV is associated with FC among DMN regions (Harms et al., 2013; Liu et al., 2020; Seidman et al., 2014). Using fMRI during cognitive task performance, Harms and colleagues (2013) found significant positive associations between HV and connectivity among regions subserving working memory in individuals with SZ, consistent with prior work (Leutgeb et al., 2007; Tamminga et al., 2010; Vargas et al., 2018). Seidman and colleagues (2014) also measured FC during task performance and found HV in first-degree relatives of SZ patients to be inversely associated with DMN activity. These findings suggest that reduced HV may be associated with impaired suppression of extraneous neural activity during cognitive tasks in SZ and genetic-risk populations.

To date, only one reported study has examined the association of HV with task-free, resting-state fMRI (rsfMRI) in SZ. Liu and colleagues (2020) examined rsfMRI using region of interest (ROI) analysis, which treats BOLD signal in a selected region as the index against which the covariation of BOLD signal at other regions is measured (Igelström & Graziano, 2017). These authors found a positive relationship between HV and hippocampal FC with the medial prefrontal cortex (mPFC) and, consistent with previous reports, HV and FC were lower in those with SZ than in healthy controls (HCs) (Liu et al., 2020). Similarly, using rsfMRI, a study of healthy adults found positive associations between HV and connectivity in the right temporoparietal junction (TPJ) (De Marco et al., 2019). fMRI studies have demonstrated that the mPFC and TPJ, which includes the overlapping inferior parietal lobule (IPL), are major hubs in the DMN (Igelström & Graziano, 2017).

As mentioned above, reductions in HV are attributed to progressive declines in inhibitory GABAergic interneurons (Benes & Berretta, 2001), which synchronize the firing patterns of excitatory pyramidal cells (Cauli et al., 2004). Given the exploratory nature of this work, and the difficulties disambiguating confounding effects of task performance from baseline hemodynamics in task-based fMRI (Thomason et al., 2013; Wink et al., 2006),

associations between HV and hippocampal FC were examined during rsfMRI in the present study. Examining this association in individuals at CHR-P is especially important, given that prior work has demonstrated that global declines in brain network modularity are driven by aberrations within the DMN as psychosis develops (Cao et al., 2020) and the DMN is reliably evoked during rsfMRI (Buckner & DiNicola, 2019). Informed by rsfMRI investigations showing positive relationships between DMN connectivity and HV in HCs and those with SZ (De Marco et al., 2019; Liu et al., 2020), the present study examined the associations of HV and hippocampal FC with DMN regions in HCs and those at CHR-P. Considering previous reports (De Marco et al., 2019; Liu et al., 2020), we predicted that HV would be positively associated with hippocampal FC in the DMN during rsfMRI in both CHR-P and HC participants. Moderation analyses tested whether relationships between hippocampal FC and HV were moderated by diagnostic group. *Post hoc* analyses tested the moderating role of biological sex.

Transparency and Openness

Preregistration

None of the studies or analyses included in this report were preregistered.

Data, Materials, Code, and Online Resources

The FMRIB Software Library (FSL) and FreeSurfer are both freely and publicly available, and procedures are well-characterized in software documentation. The Standard Parametric Mapping (SPM) software is a free but copyrighted software called from MATLAB, which is licensed. SPM default settings are also well-documented. The MATLAB and R code used for all analyses in this report are reproducible and available upon request from the corresponding author.

Reporting

This study involved an analysis of existing data rather than new data collection.

Ethical Approval

This work with human participants adheres to the 2013 Declaration of Helsinki. All procedures were approved and all participants provided consent (or parental assent where appropriate) in accordance with relevant guidelines and regulations at participating sites.

Methods

Sample

The study sample included participants between the ages of 12 and 30 years from the second phase of the North American Prodrome Longitudinal Study (NAPLS 2). The participants included in this study were those who had completed an MRI scan with an acquired T1-weighted structural image and rsfMRI data that passed well-documented quality assurance metrics ($N = 389$) (Cannon et al., 2015). This sample included 141 HCs, 218 non-converters (CHR-NCs) and 28 converters (CHR-Cs). All CHR-P participants met criteria for attenuated positive symptom syndrome (APSS) on the Structured Interview

for Psychosis Risk Syndromes (SIPS, v5.6, 2014) at baseline, and all CHR-P participants completed the two-year follow-up visit coincident with completion of NAPLS 2. Meeting criteria for brief intermittent psychotic syndrome (BIPS) or genetic risk and functional decline (GRFD)—the two other major classifications in the SIPS—were not grounds for exclusion; however, there were very few GRFD subjects without APSS and none of whom had complete functional and structural MRI data. Similarly, there were no subjects with BIPS who had complete MRI data. Data collection for NAPLS 2 is completed, hence CHR-NCs were retrospectively categorized in the present study to include 60 APSS remitters (met APSS criteria at baseline but remitted by study completion), 70 APSS persistence (met APSS criteria at baseline and symptoms neither remitted nor progressed), and 90 APSS progression (met APSS criteria at baseline and symptoms worsened). CHR-Cs ($n = 28$) met criteria for a score of 6 (severe and psychotic) on at least one positive symptom subscale of the SIPS at or before the two-year follow-up. The aims, recruitment methods, and inclusion criteria have been described elsewhere (Addington et al., 2012; Addington et al., 2015). Demographic characteristics of the present sample are presented in Table 1.

Imaging Paradigm and Data Acquisition

Details on data acquisition and processing have been described in previous reports (Cao et al., 2020). Briefly, all participants underwent a 5-minute eyes-open rsfMRI scan (154 whole-brain volumes). Functional images were collected using gradient-recalled-echo echo-planar imaging (GRE-EPI) sequences: TR/TE 2000/30ms, 77-degree flip angle, 30 4mm slices, 1mm gap, 220mm FOV. Preprocessing was performed using the standard procedures implemented in SPM12. The hippocampus was automatically segmented from structural brain images using FSL First (Patenaude et al., 2011) and processed using FreeSurfer version 5.2 (Fischl, 2002). HV measures were adjusted for site and estimated intracranial volume, consistent with prior work suggesting that HV is highly correlated with intracranial volume (Voevodeskaya et al., 2014). Measures of HV were reliable across MRI scanners used in this study (Cannon et al., 2014).

Construction of Correlation Matrices

The processing pipeline of rsfMRI data followed that of previously published work (Cao et al., 2020). In brief, mean BOLD signal time series for each of the 116 brain regions defined by the Automated Anatomical Labeling (AAL) atlas (Tzourio-Mazoyer et al., 2002) were extracted from the preprocessed data and further corrected for movement, scanner noises, and white matter and cerebrospinal fluid signals. BOLD signal time series were bandpass filtered at 0.008-0.1 Hz. Pairwise Pearson correlation coefficients were calculated between the processed time series of each region, resulting in a 116x116 correlation matrix for each participant.

Matrix Manipulation

$N = 389$ 116x116 pairwise Pearson correlation matrices were loaded into Matlab version 2019b to create an aggregate 116x116x389 matrix. The rows corresponding to bilateral hippocampal FC with all other elements of the matrix were pulled, respectively, creating two 1x116x389 matrices. The singular dimension was removed from each matrix, and the resulting 116x389 matrices were transposed so that each row corresponded to a single

participant and each column corresponded to FC between right or left hippocampus, respectively, and all other elements of the matrix (i.e., one 389x116 matrix for right hippocampal FC and one 389x116 matrix for left hippocampal FC). The column corresponding to seed (i.e., right or left hippocampus, respectively) FC with itself (a column of 1s) was removed from both matrices, creating two 389x115 matrices. Next, the DMN regions were maintained ($n = 28$): *1)* bilateral medial superior frontal cortices, *2)* orbitofrontal cortices, *3)* anterior cingulate cortices, *4)* posterior cingulate cortices, *5)* parahippocampal gyri, *6)* inferior parietal lobule, *7)* angular gyri, *8)* precuneus, *9)* caudate, *10)* putamen, *11)* thalamus, *12)* superior temporal poles, *13)* middle temporal poles, and *14)* middle temporal gyri (Manned et al., 2010; Mevel et al., 2011; Raichle et al., 2001; Zhao et al., 2007). Thus, two 389x28 matrices were created.

Statistical Analysis

These two matrices containing pairwise Pearson correlation coefficients for bilateral hippocampal FC with DMN regions were loaded into R version 4.1 (R Core Team, 2021, Vienna). Pearson's *r*s were transformed to Fisher's *z* statistic for normalization. Vectors corresponding to matched individual bilateral HV and diagnostic group (coded as an unordered factor where 0 = HC, 1 = APSS remitter, 2 = APSS persistence, 3 = APSS progression, and 4 = CHR-C) were loaded into R using base package tools. One-way analyses of variance tested for diagnostic group differences in hippocampal FC with DMN regions and HV, respectively. Using separate loops for matrix regression, bilateral HV was regressed onto ipsilateral and contralateral hippocampal FC with each DMN region (left ipsilateral = left HV and left FC, left contralateral = left HV and right FC, right contralateral = right HV and left HC, right ipsilateral = right HV and right FC). Analyses examining the moderating role of diagnostic group included main effects for FC and group and an interaction term (group*hippocampal FC). *Post hoc* analyses examining the moderating role of biological sex included main effects for FC and sex and an interaction term (sex*hippocampal FC). A final layer of analyses tested for a three-way interaction (group*sex*hippocampal FC).

Across all regression models, unstandardized coefficients were bootstrapped with 10,000 samples using the *residual* method of the *Boot* function, which relies on the *car* (Fox & Weisberg, 2019) and *boot* (Canty & Ripley, 2021) packages in R, and which resamples residuals rather than cases to treat predictors as fixed (Fox & Weisberg, 2019). This method was chosen as cases were fixed with respect to the parent connectivity matrices from which they were derived. Bias-corrected 95% confidence intervals were constructed using the *bca* method of the *confint* function of the *car* package (Fox & Weisberg, 2019). Significance levels were adjusted for multiple comparisons using the Benjamini-Hochberg method at $p < .05$ (Benjamini & Hochberg, 1995). Standardized residuals were examined using the *stdres* function of the *MASS* package in R (Venables & Ripley, 2002). Cook's distance was examined to reveal whether any cases exerted undue influence on respective models using base package tools.

Results

One-way analyses of variance revealed no significant diagnostic group differences in FC between bilateral hippocampus and DMN regions. As reported previously on this sample, there were also no significant group differences in bilateral HV (Cannon et al., 2015). Results of tests of simple linear relationships between HV and hippocampal FC in the full sample are shown in Figure 1, and all nominally significant results are presented in Table 2. In all nominally significant cases, the relationship of HV with FC was inverse, such that lower HV was associated with greater hippocampal FC. This pattern of nominally significant findings, including the same regional associations, was also observed in *post hoc* analyses after excluding participants on antipsychotic medication at baseline ($n = 41$). Findings are summarized in Supplemental Figure S1 and Table S1.

Subsequent analyses tested whether the relationship between hippocampal FC and HV was moderated by diagnostic group. All nominally significant results are presented in Table 3, and all results that survived correction for multiple comparisons are illustrated in Figure 2. Figure 2A illustrates the relationship between left hippocampal-right IPL FC and left HV modeled separately by diagnostic group. Across all diagnostic groups, with exception of CHR-C, the association between left hippocampal-right IPL FC and left HV was inverse and not significant. There was a significant and positive relationship between these variables in CHR-C, $F(1,26) = 5.34$, $p = .029$. Similarly, across all groups with exception of CHR-C, the relationship between left hippocampal-right IPL FC and right HV was inverse. Here, there was a significant, inverse relationship between these variables in HC, $F(1,139) = 4.60$, $p = .034$. This association was positive and not significant in CHR-C. These findings are illustrated in Figure 2B.

Figure 2C illustrates the relationship between right hippocampal-left IPL FC and right HV modeled separately by diagnostic group. Again, the relationship between right hippocampal-left IPL FC and right HV was inverse across all diagnostic groups with exception of CHR-C, in which the observed relationship between these variables was positive. Here, the observed relationship was significant in APSS progression, $F(1,88) = 6.55$, $p = .012$. The same pattern of findings was observed when the significant interaction between right hippocampal-right IPL FC and right HV was modeled separately by diagnostic group, such that an inverse relationship was observed across all groups with exception of CHR-C. Here, the relationship was significant and inverse in APSS remitters, $F(1,58) = 5.81$, $p = .019$, and significant and positive in CHR-Cs, $F(1,26) = 4.08$, $p = .054$. These findings are illustrated in Figure 2D. Again, when the relationship between right hippocampal-right IPL FC and left HV was modeled separately by diagnostic group, an inverse relationship was observed across all groups with exception of CHR-C. Here, the relationship was significant and inverse in APSS remitters, $F(1,58) = 4.04$, $p = .049$, and significant and positive in CHR-Cs, $F(1,26) = 4.20$, $p = .051$, illustrated in Figure 2E.

Several findings from moderation analyses survived correction for multiple comparisons and did not include the bilateral IPL. The relationship between right hippocampal-left caudate FC and left HV was significantly moderated by diagnostic group. Here, the same general pattern of findings was observed when this relationship was modeled separately

by diagnostic group, with exception of the relationship between right hippocampal-left caudate FC and left HV in APSS remitters. The relationship was positive and not significant in this group, $F(1,58) = .01$, $p = .959$. The relationship was inverse in all other groups except for CHR-C, in which the observed relationship was positive. The relationship was not significant across all diagnostic groups (Figure 2F). The relationship between left hippocampal-right middle temporal pole FC and right HV was also modeled separately by diagnostic group. Again, there were inverse relationships between these variables in all diagnostic groups with exception of CHR-C, and a positive relationship between these variables in CHR-C. These relationships were not significant across all diagnostic groups (Figure 2G). In addition, the relationship between right hippocampal-left thalamic FC and right HV was significantly moderated by diagnostic group. Here, a discrepant pattern of findings was observed. The relationship between right hippocampal-left thalamic FC and right HV was inverse in HC, APSS remitters, and APSS progression. These relationships were not significant. The relationship was positive and not significant in APSS persistence, and inverse and not significant in CHR-C (Figure 2H).

We also re-examined the moderating role of diagnostic group after excluding participants on antipsychotic medication at baseline. The results of these moderation analyses are outlined in Supplemental materials and summarized in Table S2. Briefly, the pattern of findings observed in that subsample indicated that hippocampal FC with the superior temporal pole and posterior cingulate cortex (PCC) were associated with HV. None of the relationships were significant when the interaction terms were modeled separately by diagnostic group (Figure S2).

Post hoc analyses also revealed that the relationship between hippocampal-left middle temporal pole FC and HV was significantly moderated by biological sex in the left ipsilateral and left contralateral models. Upon further examination, the association between left hippocampal-left middle temporal pole FC and left HV was positive and not significant in males, and inverse and not significant in females. The association between right hippocampal-left middle temporal pole FC and left HV was inverse and not significant in both males and females. Across all regression models, the three-way interaction between group, sex, and hippocampal FC was not significant.

Finally, *post hoc* analyses, guided by observed differences in specific demographic variables by diagnostic group (Table 1), examined whether years of education, maternal education score, or race/ethnicity were associated with bilateral HV or hippocampal FC. There were no significant differences in bilateral HV or hippocampal FC with DMN regions by race or ethnicity (Table S3). Years of education (Table S4) and maternal education score (Table S5) were not correlated with bilateral HV or hippocampal FC with exception of an observed correlation between years of education and right hippocampal FC with the left, $r(386) = 0.10$, $p = .049$, and right, $r(386) = 0.11$, $p = .023$, anterior cingulate cortex.

Discussion

Contrary to our hypothesis that HV would be positively associated with hippocampal FC in the DMN during rsfMRI, in the full sample we observed significant inverse relationships

between HV and hippocampal FC with the IPL and thalamus. These results were largely unchanged when those at CHR-P on antipsychotic medication were excluded from analysis. There were significant diagnostic group differences in the relationships between bilateral HV and bilateral hippocampal FC with the IPL, temporal pole, and PCC, which were influenced by the inclusion of participants taking antipsychotic medication.

Specifically, when the full sample of individuals at CHR-P was included in analysis, inverse relationships between hippocampal-IPL FC and HV were detected in HCs and those at CHR-P who did not develop psychosis (remittance, persistence, and progression), but positive relationships between hippocampal-IPL FC and HV were observed in individuals at CHR-P who developed clinical symptoms of psychosis during the NAPLS 2 study follow-up period. Similarly, when individuals at CHR-P on antipsychotic medication were excluded from analysis ($n = 41$), inverse relationships between hippocampal-temporal pole FC and HV were detected in HCs. However, positive relationships between hippocampal-temporal pole FC and HV were observed across groups at CHR-P.

Conversely, we observed positive relationships between hippocampal-PCC FC and HV in HCs, and inverse relationships between these variables in groups at CHR-P when those at CHR-P on antipsychotic medication were excluded. It is important to note that several of the associations between hippocampal-IPL FC and HV were significant when modeled separately by diagnostic group, yet none of the relationships between hippocampal-temporal pole FC or hippocampal-PCC FC and HV were significant when modeled separately by group. Critically, the IPL and superior temporal pole are components of the temporoparietal junction (TPJ), a variably defined region located roughly where the IPL meets the superior temporal pole, which is largely expanded in humans relative to non-human primates and understood to be a hub of an integrative multinetwork system (Igelström & Graziano, 2017).

It is also important to note that our findings from the full sample suggested that CHR-Cs had aberrant associations between hippocampal-IPL FC and HV relative to HCs and other CHR-P groups, yet CHR-Cs were not the only group at CHR-P that included participants taking antipsychotic medication at baseline. Seventeen percent of individuals at CHR-P in the present sample were taking antipsychotic medication—$n = 9$ APSS remitters, $n = 15$ APSS persistence, $n = 10$ APSS progression, and $n = 7$ CHR-Cs—a proportion consistent with observations from other cohort studies of youth at-risk for psychosis (Mensi et al., 2021). Participant exposure to antipsychotic medication is an established confound in the FC literature (Duan et al., 2020; Gratton & Mittal, 2020) largely due to the modulatory role of medication in neuronal firing patterns.

For example, Dzyubenko and colleagues (2017) exposed hippocampal cells to first- and second-generation antipsychotic medication *in vitro*. These authors demonstrated that haloperidol dampened excitatory neural activity and reduced synchrony between excitatory and inhibitory cell populations, and olanzapine increased both excitatory activity and coordination of neural activity between cell populations. Modulation of the excitation/inhibition balance has downstream consequences for the fluctuations in neural activity that contribute to BOLD signal observed during rest, which has further consequences for the regional correlations in BOLD signal that comprise FC relations (Cauli et al., 2004;

Lecrux et al., 2011). Of course, other factors (e.g., cerebral blood flow and volume) influence BOLD signal (Hillman, 2014). It is beyond the scope of the current study to elucidate the primary contributing factor to the shift in the pattern of findings observed when individuals on antipsychotic medication were excluded from analysis. Indeed, differentiating the iatrogenic effects of antipsychotic treatment from the underlying syndrome is not so straightforward in observational studies of individuals at CHR-P.

Importantly, irrespective of whether participants taking antipsychotic medication were included, this work implicates the IPL and temporal pole, or TPJ more broadly, as sensitive to differences in HV. Similar to the PCC, the TPJ is considered a core functional hub of the DMN (Igelström & Graziano, 2017). Indeed, this work adds to a growing body of limited research on associations between HV and connectivity that implicates functional hubs (Igelström et al., 2015) of the DMN including the IPL, PCC, TPJ (De Marco et al., 2019), and mPFC (Liu et al., 2020). Alterations in the connectivity of functional hubs is consistent with the dysconnectivity hypothesis of SZ, which suggests that psychotic disorder is characterized by reductions in the connections of functional hubs and dysconnectivity among brain regions (Fornito et al., 2012). An overwhelming majority of studies of DMN connectivity in individuals with SZ and other chronic psychoses have reported evidence for reduced DMN connectivity in affected individuals (Bluhm et al., 2007; Fornito et al., 2012; Jang et al., 2011; but see Fox et al., 2017; Zhou et al., 2007), and there is evidence that functional brain networks become more diffuse as psychosis develops (Cao et al., 2020; Fornito et al., 2012). To our knowledge, this work represents the first effort to characterize the HV to connectivity interface in prodromal psychoses. Given the pattern of findings, and consistent with prior work (Liu et al., 2020; De Marco et al., 2019), it is plausible that HV and hippocampal FC are meaningfully linked.

Consistent with that notion, experimental animal models have provided support for a bidirectional relationship between HV and hippocampal FC. In an experimental study of rhesus monkeys with and without neonatal hippocampal lesions, follow-up MRI confirmed that the lesioned animals had smaller HV and revealed that bilateral hippocampal FC with the dorsolateral and ventrolateral prefrontal cortices differed between lesioned and control animals. The association between HV and hippocampal FC with those frontal regions was positive in the control animals and inverse in the lesioned group, and the magnitude of the right hippocampal FC relation with the bilateral dorsolateral prefrontal cortex was significantly associated with the extent of the hippocampal lesion. The authors suggested that hippocampal lesion and consequent reduction in HV resulted in functional brain network reorganization (Li et al., 2021).

In contrast, there is experimental evidence that reduced hippocampal FC may sometimes be an antecedent of reductions in HV. Rodent models of stress-induced changes in brain function and structure have demonstrated that aberrant FC in a brain network involving the hippocampus and thalamus precedes stress-related declines in HV (Magalhães et al., 2018). Consistent with this assumption, recent clinical research revealed that, compared to HCs, adolescents with posttraumatic stress disorder (PTSD) had reduced hippocampal FC to the DMN but did not differ significantly from HCs in HV (Sussman et al., 2022). This research

suggests that hippocampal FC changes may precede reductions in HV that are typically observed in PTSD (Woon et al., 2010).

The relationships between hippocampal-IPL FC and HV were significantly moderated by diagnostic group across all regression models tested in the present study. Supplemental moderation analyses, which excluded participants taking antipsychotic medications, resulted in a distinct pattern of findings that implicated the superior temporal pole and PCC. As mentioned previously, the TPJ and PCC are considered core functional hubs of the DMN (Igelström & Graziano, 2017). Critically, independent components analysis (ICA) of BOLD signal localized to the TPJ has revealed that the intersection between the posterior IPL and temporal lobe represents a reliable subdivision of the TPJ characterized by robust connections to the DMN, and especially the precuneus and mPFC—other core hubs of the DMN. Indeed, rsfMRI studies have revealed the existence of at least four reliable subdivisions of the bilateral TPJ that each maintain specialized connectivity patterns (Igelström & Graziano, 2017). The division relevant to the current work, including the IPL and temporal pole, is intricately connected to one of two subsystems of the DMN—the medial temporal subsystem—which includes the hippocampus and connects to the other subsystem via the mPFC and PCC (Igelström et al., 2015; Igelström & Graziano, 2017; Seidman et al., 2014).

There are several reasons to expect that hippocampal connectivity with the medial temporal subsystem would have particular relevance. The hippocampus and IPL appear to have similar activation properties. In an fMRI study that employed both resting state and task-based methods, Smith and colleagues (2018) demonstrated that, unlike other regions in the medial temporal subsystem that activated at task-switching or task initiation, the hippocampus and IPL activated only at the initiation or continuation of resting state (see Supplement in Smith et al., 2018). These findings suggest that the hippocampus and IPL may be especially intricately connected, even within a specialized subsystem of the DMN.

The medial temporal subsystem is heavily implicated in self-referential decision-making and judgments about the present (Smith et al., 2018), and it has been shown to activate strongly when individuals are exposed to simulations of losses of agency (Igelström & Graziano, 2017). This subsystem, together with the precuneus and PCC, is also activated during belief reasoning tasks (Igelström & Graziano, 2017), such as the false belief task (Saxe & Kanwisher, 2003). Relatedly, some of the earliest disruptions in neural circuitry implicated in psychosis spectrum disorders are within systems responsible for indexing experience by time, place, and agency, which suggests that affected individuals fail to recognize their thoughts as self-generated or constrain their interpretations to be consistent with prior experiences (Cannon, 2015). While speculative at this juncture, the current findings may suggest that aberrant hippocampal FC with this subsystem leads to faulty recruitment of autobiographical memories from the hippocampus and a degraded sense of agency modulated by relevant connections to parietal and temporal regions, which precipitates odd or delusional beliefs that become instantiated during the progression to florid psychosis as the hippocampus atrophies and brain networks become more diffuse.

Still, we are careful to point out that there are differences between the pattern of findings revealed in the full sample and with moderation by diagnostic group. There was a significant relationship between right hippocampal-left thalamic FC and left HV in the full sample, yet the relationship between right hippocampal-left thalamic FC and right HV was significantly moderated by diagnostic group. Importantly, the moderating role of diagnostic group in the relationship between right hippocampal-left thalamic FC and left HV was not nominally significant, suggesting that hippocampal-thalamic FC is associated with HV in both HCs and individuals at CHR-P. Regarding the relationship of HV with hippocampal-thalamic FC, it is possible that the associations detected in the present study reflect compensatory processes associated with allostasis. In the present study, increased connectivity between the right hippocampus and left thalamus was significantly associated with lower left HV in the full sample. This inverse relationship may be related to the essential role of the thalamus for resource allocation and information transfer in the brain (Schiff, 2008). A recent study of associations between stress reactivity and brain network organization found increased network centrality in the thalamus to be significantly associated with higher subjective stress ratings during a laboratory stress task, and there were positive correlations among thalamic network centrality, heart rate, and salivary cortisol (Reinelt et al., 2019). It has been suggested that increased network centrality in the thalamus reflects increased alertness (Zhu et al., 2018), so perhaps greater hippocampal FC with the thalamus reflects an adaptive change reflecting the importance of remaining vigilant in anticipation of subsequent stressors.

Indeed, while speculative, it is possible that the associations observed between hippocampal FC and HV in the present study reflect the influence of stress exposure. For example, the robust relations observed between the hippocampus and IPL in this study may be related to the IPL's sensitivity to adverse environmental influence, similar to the hippocampus (e.g., Davis et al., 2017; Merz et al., 2019; Zheng et al., 2021). Research has found inverse associations between allostatic load (i.e., a quantified index of multiple stress indicators) and IPL thickness in both healthy individuals and those with SZ (Chiappelli et al., 2017). Moreover, the IPL matures late in human development (Igelström & Graziano, 2017; Shenton et al., 2001). While phylogenetically older, the hippocampus also has a protracted developmental course (Carrion et al., 2007; Chen & Baram, 2016). It is possible that hippocampal-IPL connectivity is strongly associated with HV due in part to their shared protracted development and sensitivity to prolonged exposure to stress.

An important future direction of this work will be to determine the role of stress exposure and neurobiological indices of the stress response, such as cortisol levels, on relationships between brain morphometry and connectivity. Heritability estimates for HV are modest compared to those for other brain regions (e.g., 40% heritability for HV vs 88% heritability for cerebellar volume) (Peper et al., 2007), and reductions in HV are associated with prolonged exposure to stress and other adverse experiences in both humans and non-human animals (Burrage et al., 2018; Schobel et al., 2013). Further work is needed to elucidate the complex interplay between endogenous cortisol, exposure to stress, hippocampal connectivity, and HV. Indeed, in individuals with major depressive disorder, also characterized by reductions in HV (Chen et al., 2020), heightened cortisol levels have been associated with increased cortico-cerebellar connectivity patterns (Wang et al.,

2018). Measures of stress reactivity, including levels of endogenous cortisol, should be considered in future investigations of the HV to connectivity interface, especially as cortisol binds preferentially in the hippocampus (Benes & Berretta, 2001). In addition, measures of sex hormones may be considered in future investigations of this interface. We observed limited asymmetries in the association between hippocampal-middle temporal pole FC and HV between the sexes, which may be related to the influence of sex hormones in the hippocampus. Neuronal spine density and synaptic plasticity in the hippocampus have been shown to be sensitive to estrogen—an effect not seen in the cortex nor cerebellum (Fester & Rune, 2021). We emphasize that there is no published basis for theorizing about the nature of associations between hippocampal FC and HV between the sexes.

There are several limitations to the present study. There is strong theoretical backing for selecting the hippocampus as an ROI (Kremen et al., 2010; Peper et al., 2007), but ROI analyses are influenced by the position of the selected region (Igelström & Graziano, 2017). Further, the present study is cross-sectional. While this is a critical first step, longitudinal work will be needed to establish temporal precedence between changes in HV and hippocampal FC, particularly as reductions in HV may be partially reversible in clinical populations (Hou et al., 2020). Longitudinal research also holds promise for shedding light on neural mechanisms underlying the observed relationships, especially whether other variables, including adrenal or gonadal hormones, moderate these relationships. Another limitation to the present study is that geographic location of origin information was not included. HV has been shown to be sensitive to many environmental insults, including air pollution (Hedges et al., 2019). Neighborhood characteristics, including socioeconomic deprivation, have also been associated with reductions in HV (Ku et al., 2022) and greater incidence and prevalence of psychosis even after accounting for genetic risk (Anglin et al., 2021; Newbury et al., 2020). Both individual-level (e.g., cortisol) and environmental-level (e.g., percentage of residents living below the poverty line) indicators of stress may be considered in future research that elucidates the role of stress in the relationships observed in the present study.

To summarize, our findings indicate that hippocampal connectivity with the IPL and thalamus is inversely associated with HV in both healthy individuals and those at CHR-P. In addition, we observed significant moderation of the relationship between hippocampal-IPL FC and HV by diagnostic group, such that a positive association between these variables was observed in individuals who ultimately developed psychosis. This work broadly indicates that hippocampal FC with a reliable subdivision of the TPJ, which includes the IPL and superior temporal pole, is associated with HV. Future investigations of links between hippocampal connectivity and volume may elucidate the organization of specialized subsystems within the DMN, or the influence of a common factor, such as exposure to stress, that alters both brain function and structure.

Supplementary Material

Refer to Web version on PubMed Central for supplementary material.

Funding

References

Addington J, Liu L, Cadenhead KS, Cannon TD, Cornblatt BA, Perkins DO …& McGlashan TH (2015). North American Prodrome Longitudinal Study (NAPLS 2): The prodromal symptoms. Journal of Nervous and Mental Disorders 203(5), 328–335.

Addington J, Cadenhead KS, Cornblatt BA, Mathalon DH, McGlashan TH, Perkins DO, …& Cannon TD (2012). North American Prodrome Longitudinal Study (NAPLS 2): Overview and recruitment. Schizophrenia Research 142, 77–82.

Andrews-Hanna JR, Reidler JS, Sepulcre J, Poulin R, & Buckner RL (2010). Functional-anatomic fractionation of the brain's default network. Neuron, 65, 550–562.

Anglin DM, Ereshefsky S, Klaunig MJ, Bridgwater MA, Niendam TA, Ellman LM, … & van der Ven E (2021). From womb to neighborhood: A racial analysis of social determinants of psychosis in the United States. American Journal of Psychiatry, 178(7), 599–610.

Bassett DS, & Sporns O (2017). Network neuroscience. Nature, 20(3), 353–364.

Benes FM, & Berretta S (2001). GABAergic interneurons: Implications for understanding schizophrenia and bipolar disorder. Neuropsychopharmacology, 25, 1–27.

Benjamini Y, & Hochberg Y (1995). Controlling the false discovery rate: A practical and powerful approach to multiple testing. J R Stat Soc, 57, 289–300.

Bluhm RL, Miller J, Lanius RA, Osuch EA, Boksman K, Neufeld RW, … & Williamson P (2007). Spontaneous low-frequency fluctuations in the BOLD signal in schizophrenic patients: Anomalies in the default network. Schizophrenia Bulletin, 33(4), 1004–1012.

Buckner RL, & DiNicola LM (2019). The brain's default network: Updated anatomy, physiology and evolving insights. Nature Reviews Neuroscience, 20, 593–608.

Burrage E, Marshall KL, Santanam N, & Chantler PD (2018). Cerebrovascular dysfunction with stress and depression. Brain Circulation, 4(2), 43.

Cabral J, Hugues E, Sporns O, & Deco G (2011). Role of local network oscillations in resting-state functional connectivity. Neuroimage, 57, 130–139.

Cannon TD (2015). How schizophrenia develops: Cognitive and brain mechanisms underlying onset of psychosis. Trends in Cognitive Sciences, 19(12), 744–756.

Cannon TD, Chung Y, He G, Sun D, Jacobson A, van Erp TG, … & Heinssen R (2015). Progressive reduction in cortical thickness as psychosis develops: a multisite longitudinal neuroimaging study of youth at elevated clinical risk. Biological Psychiatry, 77(2), 147–157.

Cannon TD, Sun F, McEwen SJ, Papademetris X, He G, van Erp TGM, Jacobsen A, … & Toga AW (2014). Reliability of neuroanatomical measurements in a multisite longitudinal study of youth at risk for psychosis. Human Brain Mapping, 35(5), 2424–2434.

Canty A, & Ripley B (2021). Boot: Bootstrap R (S-Plus) functions. R package version 1.3-26.

Cao H, Chung Y, McEwen SC, Bearden CE, Addington J, Goodyear B, … & Cannon TD (2020). Progressive reconfiguration of resting-state brain networks as psychosis develops: Preliminary results from the North American Prodrome Longitudinal Study. Schizophrenia Research, 226, 30–37.

Carrion VG, Weems CF, & Reiss AL (2007). Stress predicts brain changes in children: A pilot longitudinal study on youth stress, posttraumatic stress disorder, and the hippocampus. Pediatrics, 119, 509–516.

Cauli B, Tong X, Rancillac A, Serluca N, Lambolez B, Rossier J, & Hamel E (2004). Cortical GABA interneurons in neurovascular coupling: Relays for subcortical vasoactive pathways. Journal of Neuroscience, 24(41), 8940–8949.

Chen F, Bertelsen AB, Holm IE, Nyengaard JR, Rosenberg R, & Dorph-Petersen K (2020). Hippocampal volume and cell number in depression, schizophrenia, and suicide subjects. Brain Research, 1727. doi: 10.1016/j.brainres.2019.146546.

Chen Y, & Baram TZ (2016). Toward understanding how early-life stress reprograms cognitive and emotional brain networks. Neuropsychopharmacology, 41, 197–206.

Chiappelli J, Kochunov P, Savransky A, Fisseha F, Wisner K, Du X, … & Hong LE (2017). Allostatic load and reduced cortical thickness in schizophrenia. Psychoneuroendocrinology, 77, 105–111.

Davis EG, Humphreys KL, McEwen LM, Sacchet MD, Camacho MC, Maclssac JL, … & Gotlib IH (2017). Accelerated DYNA methylation age in adolescent girls: Associations with elevated diurnal cortisol and reduced hippocampal volume. Translational Psychiatry, 7(8), e1223.

De Marco M, Ourselin S, & Venneri A (2019). Age and hippocampal volume predict distinct parts of default mode network activity. Scientific Reports, 9(1). doi: 10.1038/s41598-019-52488-9.

Dickerson LW, Bonthius DJ, Schutte BC, Yang B, Barna TJ, Bailey MC, … & Lamb FS (2002). Altered GABAergic function accompanies hippocampal degeneration in mice lacking C1C-3 voltage-gated chloride channels. Brain Research, 958, 227–250.

Duan X, Hu M, Huang X, Dong X, Zong X, He C, … & Chen H (2020). Effects of risperidone monotherapy on the default-mode network in antipsychotic-naïve first-episode schizophrenia: Posteromedial cortex heterogeneity and relationship with the symptom improvements. Schizophrenia Research, 218, 201–208.

Dzyubenko E, Juckel G, & Faissner A (2017). The antipsychotic drugs olanzapine and haloperidol modify neural network connectivity and spontaneous activity of neural networks *in vitro*. Scientific Reports, 7(1): doi: 10.1038/s41598-017-11944-0.

Fester L, & Rune GM (2021). Sex neurosteroids: Hormones made by the brain for the brain. Neuroscience Letters, 753. doi: 10.1016/j.neulet.2021.135849.

Fischl B (2002). FreeSurfer. Neuroimage, 62(2), 774–781.

Fornito A, Zalesky A, Pantelis C, & Bullmore ET (2012). Schizophrenia, neuroimaging and connectomics. Neuroimage, 62, 2296–2314.

Fox JM, Abram SV, Reilly JL, Eack S, Goldman MB, Csernansky JG, … & Smith MJ (2017). Default mode functional connectivity is associated with social functioning in schizophrenia. Journal of Abnormal Psychology, 126(4), 392–405.

Fox J, & Weisberg S (2019). An R companion to applied regression. (3rd ed.). Thousand Oaks, CA: Sage.

Gong G, He Y, Concha L, Lebel C, Gross DW, Evans AC, & Beaulieu C (2009). Mapping anatomical connectivity patterns of human cerebral cortex using in vivo diffusion tensor imaging tractography. Cerebral Cortex 19, 524–536.

Gratton C, & Mittal VA (2020). Embracing the complexity of heterogeneity in schizophrenia: A new perspective from latent clinical-anatomical dimensions. Schizophrenia Bulletin, 46(6), 1337–1338.

Harms MP, Wang L, Csernansky JG, & Barch DM (2013). Structure-function relationship of working memory activity with hippocampal and prefrontal cortex volumes. Brain Structure Function, 218, 173–186.

Heckers S, & Konradi C (2015). GABAergic mechanisms of hippocampal hyperactivity in schizophrenia. Schizophrenia Research, 167, 4–11.

Hedges DW, Erickson LD, Kunzelman J, Brown BL, & Gale SD (2019). Association between exposure to air pollution and hippocampal volume in adults in the UK Biobank. Neurotoxicology, 74, 108–120.

Hillman EMC (2014). Coupling mechanism and significance of the BOLD signal: A status report. Annual Reviews in Neuroscience, 37, 161–181.

Hinney B, Walter A, Aghlmandi S, Andreou C, & Borgwardt S (2021). Does hippocampal volume predict transition to psychosis in a high-risk group? A meta-analysis. Frontiers in Psychiatry, 11, 1582.

Hou B, Gao L, Shi L, Luo Y, Guo X, Young GS, Qin L, … & Feng F (2020). Reversibility of impaired brain structures after transsphenoidal surgery in Cushing's disease: A longitudinal study based on an artificial intelligence-assisted tool. Journal of Neurosurgery. doi: 10.3171/2019.10.JNS191400.

Igelström KM, & Graziano MSA (2017). The inferior parietal lobule and temporoparietal junction: A network perspective. Neuropsychologia, 105, 70–83.

Igelström KM, Webb TW, & Graziano MS (2015). Neural processes in the human temporoparietal cortex separated by localized independent component analysis. Journal of Neuroscience, 35, 9432–9445.

Jang JH, Jung WH, Choi JS, Choi CH, Kang DH, Shin NY, … & Kwon JS (2011). Reduced prefrontal functional connectivity in the default mode network is related to greater psychopathology in subjects with high genetic loading for schizophrenia. Schizophrenia Research, 127(1), 58–65.

Kremen WS, Prom-Wormley E, Panizzon MS, Eyler LT, Fischl B, Neale MC, … & Fennema-Notestine C (2010). Genetic and environmental influences on the size of specific brain regions in midlife: The VETSA MRI study. Neuroimage, 49, 1213–1223. [PubMed: 19786105]

Ku BS, Aberizk K, Addington J, Bearden CE, Cadenhead KS, Cannon TD, … & Walker EF (2022). The association between neighborhood poverty and hippocampal volume among individuals at clinical high-risk for psychosis: The moderating role of social engagement. Schizophrenia Bulletin, 48(5), 1032–1042. [PubMed: 35689540]

Lecrux C, Toussay X, Kocharyan A, Fernandes P, Neupane S, Lévesque M, … & Hamel E (2011). Pyramidal neurons are "neurogenic hubs" in the neurovascular coupling response to whisker stimulation. Journal of Neuroscience, 31(21), 9836–9847. [PubMed: 21734275]

Leutgeb J, Leutgeb S, Moser M, & Moser E (2007). Pattern separation in the dendate gyrus and CA3 of the hippocampus. Science, 315, 961–966. [PubMed: 17303747]

Li C, Li Z, Hu X, Zhang X, & Bachevalier J (2021). Altered hippocampal-prefrontal functional network integrity in adult macaque monkeys with neonatal hippocampal lesions. Neuroimage, 15, 117645.

Liu S, Liu Y, Yan H, Wang M, Sun Y, Fan L, … & Liu B (2020). Polygenic effects of schizophrenia on hippocampal grey matter volume and hippocampus-medial prefrontal cortex functional connectivity. The British Journal of Psychiatry, 216, 267–264. [PubMed: 31169117]

Logothetis NK, & Pfeuffer J (2004). On the nature of the BOLD fMRI contrast mechanism. Magnetic Resonance Imaging, 22, 1517–1531. [PubMed: 15707801]

Magalhães R, Barrière DA, Novais A, Marques F, Marques P, Cerqueira J, … & Sousa N (2018). The dynamics of stress: A longitudinal MRI study of rat brain structure and connectome. Molecular Psychiatry, 23, 1998–2006. [PubMed: 29203852]

Mannell MV, Franco AR, Cahoun VD, Canive JM, Thoma RJ, & Mayer AR (2010). Resting state and task-induced deactivation: A methodological comparison in patients with schizophrenia and healthy controls. Human Brain Mapping 31(3), 424–437. [PubMed: 19777578]

Mensi MM, Molteni S, Iorio M, Filosi E, Ballante E, Balottin U, … & Borgatti R (2021). Prognostic accuracy of DSM-5 attenuated psychosis syndrome in adolescents: Prospective real-world 5-year cohort study. Schizophrenia Bulletin, 47(6), 1663–1673. [PubMed: 33939829]

Merz EC, Desai PM, Maskus EA, Melvin SA, Rehman R, Torres SD, … & Noble KG (2019). Socioeconomic disparities in chronic physiologic stress are associated with brain structure in children. Biological Psychiatry, 86(12), 921–929. [PubMed: 31409452]

Mevel K, Chetelat G, Eustache F, & Desgranges B (2011). The default mode network in healthy aging and Alzheimer's disease. Int J Alzheimer Disease. doi: 10.4061/2011/535816.

Modinos G, Richter A, Egerton A, Bonoldi I, Azis M, Antoniades M, … & McGuire P (2021). Interactions between hippocampal activity and striatal dopamine in people at clinical high risk for psychosis: Relationships to adverse outcomes. Neuropsychopharmacology, 46, 1468–1474. [PubMed: 33941857]

Newbury JB, Arseneault L, Caspi A, Moffitt TE, Odgers CL, Belsky DW, … & Fisher HL (2020). Association between genetic and socioenvironmental risk for schizophrenia during upbringing in a UK longitudinal cohort. Psychological Medicine. doi: 10.1017/S0033291720003347.

Patenaude B, Smith SM, Kennedy D, & Jenkinson M (2011). A Bayesian model of shape and appearance for subcortical brain. NeuroImage, 56(3), 907–922. [PubMed: 21352927]

Peper JS, Brouwer RM, Boomsma DI, Kahn RS, & Hulshoff Pol HE (2007). Genetic influences on human brain structure: A review of brain imaging studies in twins. Human Brain Mapping, 28, 464–473. [PubMed: 17415783]

Provenzano FA, Guo J, Wall MM, Feng X, Sigmon HC, Brucato G, … & Small SA (2020). Hippocampal pathology in clinical high-risk patients and the onset of schizophrenia. Biological Psychiatry, 87(3), 234–242. [PubMed: 31771861]

Raichle ME, MacLeod AM, Snyder AZ, Powers WJ, Gusnard DA, & Shulman GL (2001). A default mode of brain function. Proceedings of the National Academy of Sciences USA 98(2), 676–682.

Reinelt J, Uhlig M, Müller K, Lauckner ME, Kumral D, Schaare HL, … & Gaebler M (2019). Acute psychosocial stress alters thalamic network centrality. Neuroimage, 199, 680–690. [PubMed: 31173902]

Saxe R, & Kanwisher N (2003). People thinking about thinking people: The role of the temporoparietal junction in "theory of mind." Neuroimage, 19, 1835–1842. [PubMed: 12948738]

Schiff ND (2008). Central thalamic contributions to arousal regulation and neurological disorders of consciousness. Ann N Y Academy of Sciences, 1129, 105–118.

Schobel SA, Chaudhury NH, Khan UA, Paniagua B, Styner MA, Asllani I, … & Small SA (2013). Imaging patients with psychosis and a mouse model establishes a spreading pattern of hippocampal dysfunction and implicates glutamate as a driver. Neuron, 78, 81–93. [PubMed: 23583108]

Seidman LJ, Rosso IM, Thermenos HW, Makris N, Juelich R, Gabrieli JDE, … & Whitfield-Gabrieli S (2014). Medial temporal lobe default mode functioning and hippocampal structure as vulnerability indicators for schizophrenia: An MRI study of nonpsychotic adolescent first-degree relatives. Schizophrenia Research, 159, 426–434. [PubMed: 25308834]

Shenton ME, Dickey CC, Frumin M, & McCarley RW (2001). A review of MRI findings in schizophrenia. Schizophrenia Research, 49(2), 1–52.

Smith V, Mitchell DJ, & Duncan J (2018). Role of the default mode network in cognitive transitions. Cerebral Cortex, 28, 3685–3696. [PubMed: 30060098]

Sussman TJ, Posner J, Jackowski AP, Correa A, Hoffmann EV, Peruzzi F, … & Milani A (2022). The relationship between recent PTSD secondary to sexual assault, hippocampal volume and resting state functional connectivity in adolescent girls. Neurobiology of Stress, 17, 100441. [PubMed: 35257017]

Tamminga CA, Stan AD, & Wagner AD (2010). The hippocampal formation in schizophrenia. American Journal of Psychiatry, 167, 1178–1193. [PubMed: 20810471]

Thomason ME, Tocco MA, Quednau KA, Bedway AR, & Carré JM (2013). Idle behaviors of the hippocampus reflect endogenous cortisol levels in youth. Journal of the American Academy of Child & Adolescent Psychiatry, 52(6), 642–652. [PubMed: 23702453]

Tzourio-Mazoyer N, Landeau B, Papathanassiou D, Crivello F, Etard O, Delcroix N, …& Joliot M (2002). Automated anatomical labeling of activations in SPM using a macroscopic anatomical parcellation of the MNI MRI single-subject brain. NeuroImage 15(1), 273–289. [PubMed: 11771995]

van Erp TGM, Hibar DP, Rasmussen JM, Glahn DC, Pearlson GD, & Andreassen OA (2015). Subcortical brain volume abnormalities in 2028 individuals with schizophrenia and 2540 healthy controls via the ENIGMA consortium. Molecular Psychiatry, 21, 547–553. [PubMed: 26033243]

Vargas T, Dean DJ, Osborne KJ, Gupta T, Ristanovic I, Ozturk S, … & Mittal VA (2018). Hippocampal subregions across the psychosis spectrum. Schizophrenia Bulletin, 44(5), 1091–1099. [PubMed: 29272467]

Venables WN, & Ripley BD (2002). Modern applied statistics with R. (4th ed.). Springer: New York.

Voevodeskaya O, Simmons A, Nordenskjold R, Kullberg J, Ahlstrom H, Lind L, … & Westman E (2014). The effects of intracranial volume adjustment approaches on multiple regional MRI volumes in healthy aging and Alzheimer's disease. Front Aging Neuroscience, 6, 264.

Walter A, Suenderhauf C, Harrisberger F, Lenz C, Smieskova R, Chung Y, … & Vogel T (2016). Hippocampal volume in subjects at clinical high-risk for psychosis: A systematic review and meta-analysis. Neuroscience and Biobehavioral Reviews, 71, 680–690. [PubMed: 27773693]

Wang Y, Chen G, Zhong S, Jia Y, Xia L, Lai S, … & Liu T (2018). Association between resting-state brain functional connectivity and cortisol levels in unmedicated major depressive disorder. Journal of Psychiatry Research, 105, 55–62.

Wink AM, Bernard F, Salvador R, Bullmore E, & Suckling J (2006). Age and cholinergic effects on hemodynamics and functional coherence of human hippocampus. Neurobiology of Aging, 27, 1395–1404. [PubMed: 16202481]

Woon FL, Sood S, & Hedges DW (2010). Hippocampal volume deficits associated with exposure to psychological trauma and posttraumatic stress disorder in adults: A meta-analysis. Prog Neuropsychopharmacology Biological Psychiatry, 34(1), 1181–1188.

Zhao C, Zhu J, Liu X, Pu C, Lai Y, Chen L … & Hong N (2018). Structural and functional brain abnormalities in schizophrenia: A cross-sectional study at different stages of the disease. Prog Neuropsychopharmacology Biol Psychiatry, 83, 27–32.

Zheng Y, Garrett ME, Sun D, Clarke-Rubright EK, Haswell CC, Maihofer AX, … & Morey RA (2021). Trauma and posttraumatic stress disorder modulate polygenic predictors of hippocampal and amygdala volume. Translational Psychiatry, 11.

Zhou Y, Liang M, Tian L, Wang K, Hao Y, Liu H, … & Jiang T (2007). Functional disintegration in paranoid schizophrenia using resting-state fMRI. Schizophrenia Research, 97(1), 194–205. [PubMed: 17628434]

Zhu X, Suarez-Jimenez B, Lazarov A, Helpman L, Papini S, Lowell A, et al. (2018). Exposure-based therapy changes amygdala and hippocampus resting-state functional connectivity in patients with PTSD. Depress Anxiety 35(10), 974–984. [PubMed: 30260530]

Bilateral Hippocampal Volume with Ipsilateral and Contralateral Default Mode Network Connectivity
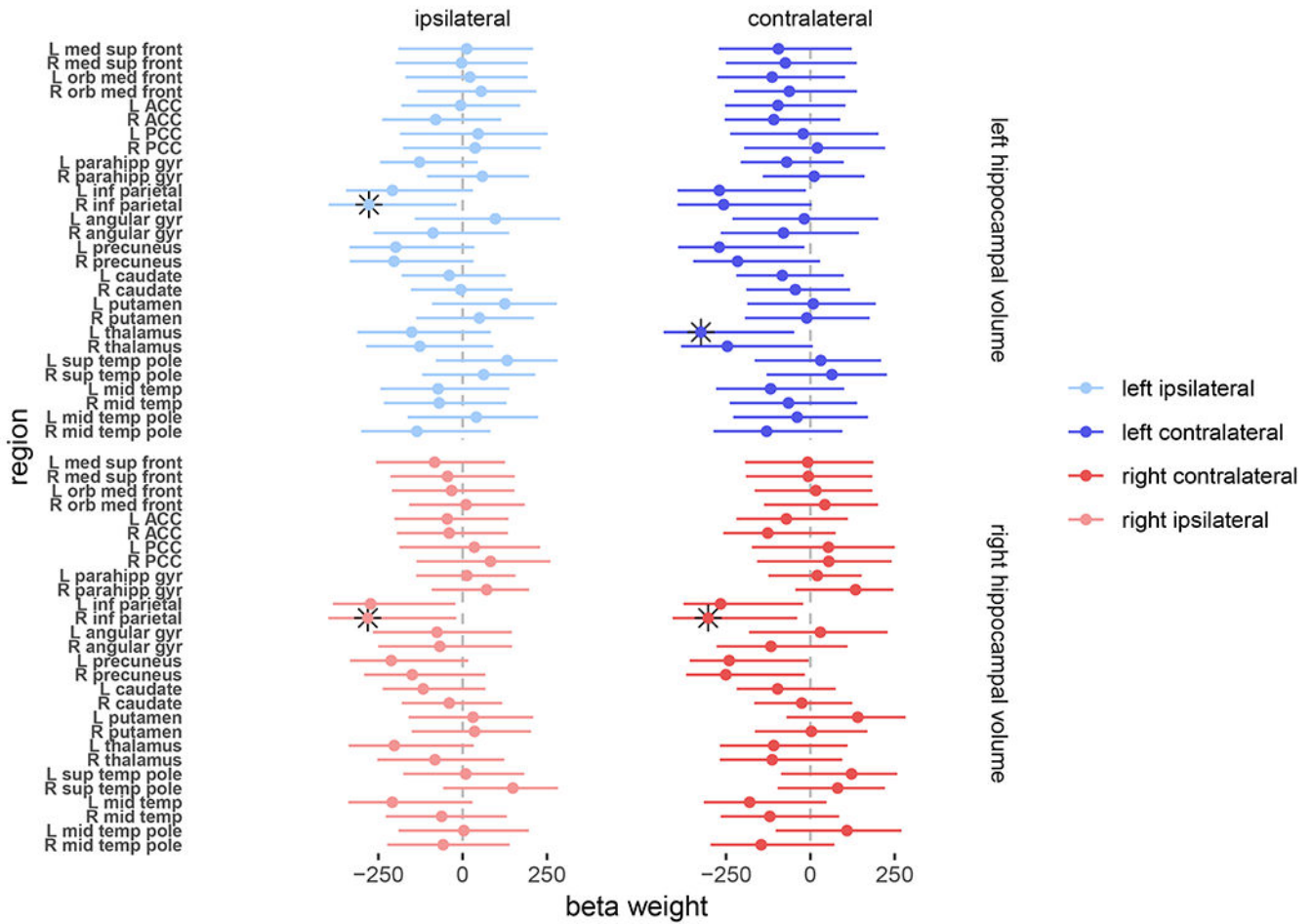
Figure 1.

Forest plot presenting the results of linear relationships between bilateral hippocampal volume (HV) and ipsilateral and contralateral default mode network connectivity. *Left ipsilateral* = left HV and left hippocampal functional connectivity (FC); *left contralateral* = left HV and right hippocampal FC; *right contralateral* = right HV and left hippocampal FC; *right ipsilateral* = right HV and right hippocampal FC; *ACC* = anterior cingulate cortex; *front* = frontal; *gyr* = gyrus; *med* = medial; *orb* = orbital; *parahipp* = parahippocampal; *PCC* = posterior cingulate cortex; *sup* = superior; *temp* = temporal. *Significant after correcting for multiple comparisons using Benjamini-Hochberg method at *p* < .05. Bootstrapped confidence intervals presented at 75% magnitude.

Figure 2.
Scatterplots present linear relationships between hippocampal functional connectivity and hippocampal volume relations that were significantly moderated by diagnostic group. In each case, the relation is modeled separately by diagnosti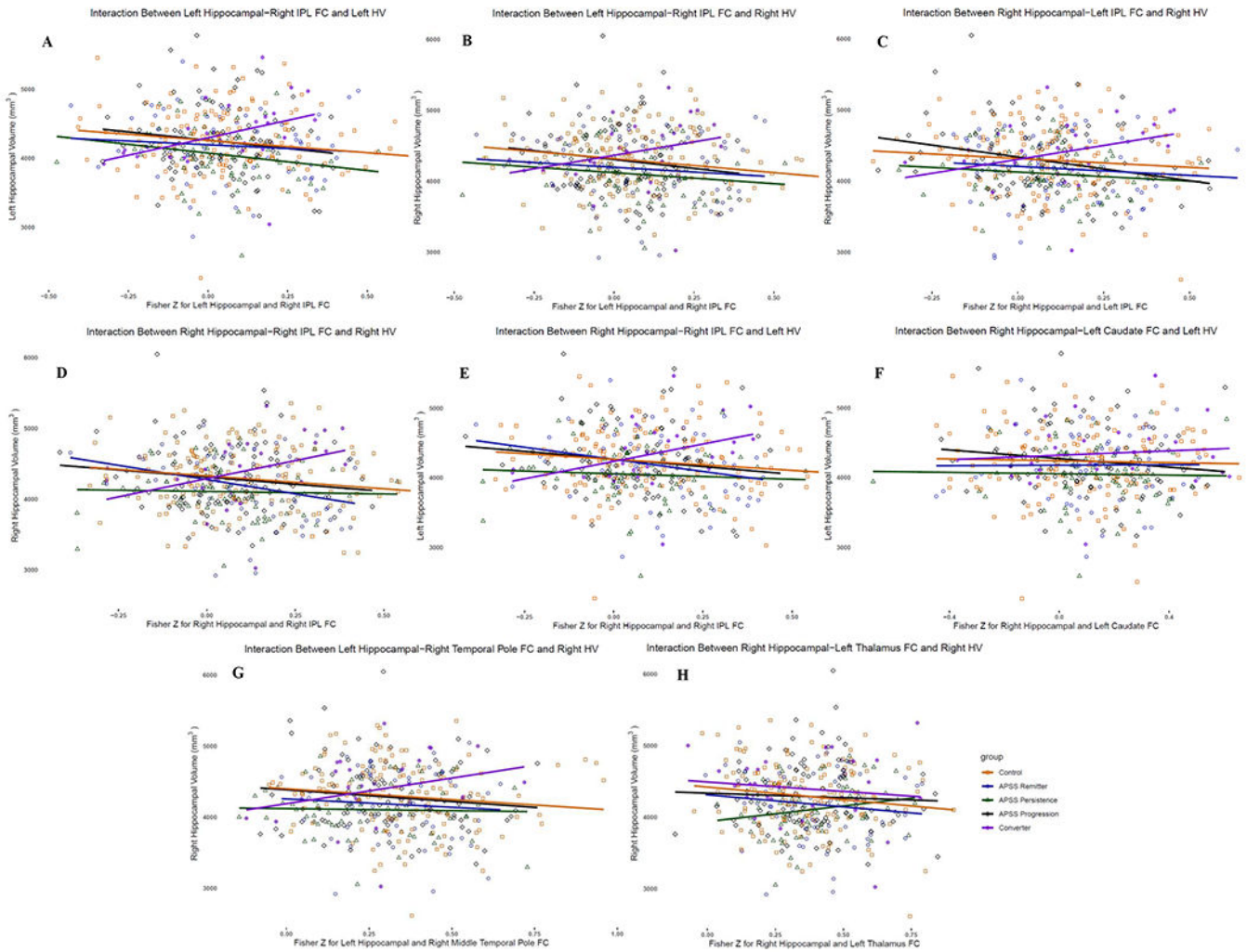c group. *APSS* = Attenuated Positive Symptom Syndrome; *FC* = functional connectivity; *HV* = hippocampal volume; *IPL* = inferior parietal lobe.

Table 1.

Demographic Characteristics

Characteristic	HC ($n = 141$)	APSS-R ($n = 60$)	APSS-Per ($n = 70$)	APSS-Pro ($n = 90$)	CHR-C ($n = 28$)	Statistical Test for Significance (2-Tailed)	P value	Post Hoc Tukey Test
Age, mean (SD)	20.3 (4.4)	18.8 (4.3)	19.9 (3.4)	19.8 (4.1)	18.9 (4.0)	$F(4) = 1.83$	.122	NA
Male sex, No. (%)	80 (56.7)	39 (65)	40 (57.1)	53 (58.9)	13 (46.4)	$\chi^2(4) = 2.88$	.578	NA
Education level, mean (SD)	12.2 (3.1)	10.7 (2.5)	12.5 (2.5)	12.0 (3.3)	12.5 (3.4)	$F(4) = 3.75$	.005 *	HC, APSS-Per > APSS-R
Paternal education score, mean (SD)	6.4 (1.8)	6.2 (1.7)	6.8 (1.6)	6.2 (1.5)	6.6 (1.8)	$F(4) = 1.59$	.177	NA
Maternal education score, mean (SD)	6.4 (1.6)	6.4 (1.6)	7.1 (1.4)	6.3 (1.6)	6.5 (1.6)	$F(4) = 3.01$	.019 *	APSS-Per > HC, APSS-Pro
Race/ethnicity, No. (%)								
White	71 (50.4)	31 (51.7)	42 (60.0)	60 (66.7)	12 (42.9)	$\chi^2(4) = 8.80$	.066	NA
Hispanic or Latino	24 (17.0)	16 (26.7)	7 (10.0)	18 (20.0)	5 (17.9)	$\chi^2(4) = 2.88$	.170	NA
Black	42 (29.8)	11 (18.3)	14 (20.0)	3 (3.3)	4 (14.3)	$\chi^2(4) = 25.46$	< .001 *	NA **
Asian	15 (10.6)	4 (6.7)	5 (7.1)	5 (5.6)	7 (25.0)	$\chi^2(4) = 3.06$	.549	NA
First Nations	0 (0)	1 (1.7)	1 (1.4)	4 (4.4)	0 (0)	$\chi^2(4) = 7.65$	.105	NA
Interracial	13 (9.2)	13 (21.7)	8 (11.4)	18 (2.0)	5 (17.9)	$\chi^2(4) = 8.56$	.073	NA
HV, mean (SD)	8489.8 (835.6)	8390.6 (914.6)	8424.7 (1026.4)	8485.9 (927.6)	8307.1 (888.03)	$F(4) = .35$	.845	NA

HC = healthy controls; $APSS\text{-}R$ = APSS Remitters; $APSS\text{-}Per$= APSS Persistence; $APSS\text{-}Pro$ = APSS Progression; $CHR\text{-}C$ = clinical high-risk converter; HV = hippocampal volume.

*
Significant at $p < .05$.

**
Adjusted residuals between expected and observed cell counts were calculated to identify the contribution of each cell to the magnitude of the significant omnibus chi-square statistic. All adjusted residuals had absolute values less than 1 with exception of that calculated for $APSS\text{-}Pro$; adjusted residual = 1.83, $p < .001$.

Table 2.

Results of nominally significant tests from matrix regression, $p < .05$, with bias-corrected 95% confidence intervals reported from bootstrapping

Version	Region	Estimate	SE	t statistic	95% CI		p value
					LL	UL	
Left ipsilateral	R inf parietal	– 277.99	128.60	– 2.16	– 529.76	– 23.68	0.031*
Left contralateral	L inf parietal	– 270.11	129.78	– 2.08	– 525.56	– 17.65	0.038
Left contralateral	L precuneus	– 270.31	125.50	– 2.15	– 522.83	– 23.69	0.032
Left contralateral	L thalamus	– 324.61	131.85	– 2.46	– 580.27	– 64.00	0.014*
Right contralateral	L inf parietal	– 266.25	122.17	– 2.18	– 501.44	– 28.67	0.030
Right contralateral	R inf parietal	– 303.04	122.98	– 2.46	– 545.13	– 52.13	0.014*
Right contralateral	L precuneus	– 240.60	119.87	– 2.01	– 477.17	– 6.27	0.045
Right contralateral	R precuneus	– 250.78	120.03	– 2.09	– 491.09	– 21.68	0.037
Right ipsilateral	L inf parietal	– 273.07	124.25	– 2.20	– 513.33	– 28.44	0.029
Right ipsilateral	R inf parietal	– 281.51	128.47	– 2.19	– 530.99	– 25.51	0.029*

Left contralateral = left HV and right hippocampal FC; *left ipsilateral* = left HV and left hippocampal FC; *right contralateral* = right HV and left hippocampal FC; *right ipsilateral* = right HV and right hippocampal FC; *inf* = inferior; *L* = left; *R* = right; *SE* = standard error; *CI* = confidence interval; *LL* = lower level; *UL* = upper level.

*
Significant after correcting for multiple comparisons.

Table 3.

Results of nominally significant tests examining the moderating role of diagnostic group, $p < .05$, with bias-corrected 95% confidence intervals reported from bootstrapping

					95% CI		
Version	Region	Estimate	SE	t statistic	LL	UL	p value
Left ipsilateral	R inf parietal	− 182.43	73.00	− 2.50	− 328.97	− 38.41	0.013 *
Left ipsilateral	L caudate	− 169.57	81.21	− 2.09	− 323.34	− 8.90	0.037
Left ipsilateral	R caudate	− 175.53	81.97	− 2.14	− 334.20	− 10.78	0.033
Left contralateral	L inf parietal	− 172.60	78.65	− 2.19	− 329.48	− 23.22	0.029
Left contralateral	R inf parietal	− 208.16	74.15	− 2.81	− 355.44	− 60.82	0.005 *
Left contralateral	L caudate	− 185.61	79.34	− 2.34	− 338.63	− 30.54	0.020 *
Left contralateral	R caudate	− 188.75	85.29	− 2.21	− 352.58	− 17.75	0.027
Right contralateral	R inf parietal	− 198.90	69.78	− 2.85	− 335.68	− 59.12	0.005 *
Right contralateral	R parahippocampal	− 391.00	185.70	− 2.11	− 753.97	− 31.22	0.036
Right contralateral	R angular gyrus	− 196.22	88.45	− 2.22	− 370.28	− 25.12	0.027
Right contralateral	R precuneus	− 222.22	106.87	− 2.08	− 429.00	− 14.56	0.038
Right contralateral	L caudate	− 172.85	77.29	− 2.24	− 321.38	− 22.21	0.026
Right contralateral	R caudate	− 166.73	78.16	− 2.13	− 317.15	− 11.17	0.034
Right contralateral	R middle temporal	− 279.48	122.24	− 2.29	− 517.93	− 37.69	0.023 *
Right ipsilateral	L orbital medial	− 210.64	103.46	− 2.04	− 418.07	− 9.52	0.042
Right ipsilateral	L parahippocampal	− 425.07	191.29	− 2.22	− 800.68	− 42.40	0.027
Right ipsilateral	R parahippocampal	− 551.05	230.25	− 2.39	− 1006.10	− 89.17	0.017
Right ipsilateral	L inf parietal	− 191.22	74.87	− 2.55	− 338.91	− 44.98	0.011 *
Right ipsilateral	R inf parietal	− 220.83	70.50	− 3.13	− 358.39	− 81.01	0.002 *
Right ipsilateral	L angular gyrus	− 187.11	81.68	− 2.29	− 347.87	− 24.56	0.023
Right ipsilateral	R angular gyrus	− 182.04	90.82	− 2.00	− 359.22	− 5.70	0.046
Right ipsilateral	L caudate	− 183.98	75.38	− 2.44	− 330.77	− 36.18	0.015
Right ipsilateral	R caudate	− 171.08	81.21	− 2.11	− 324.75	− 8.37	0.036
Right ipsilateral	L putamen	− 247.62	114.61	− 2.16	− 478.82	− 22.23	0.031
Right ipsilateral	R putamen	− 241.57	114.41	− 2.11	− 472.13	− 19.75	0.035
Right ipsilateral	L thalamus	− 482.63	162.43	− 2.97	− 789.01	− 156.62	0.003 *
Right ipsilateral	R thalamus	− 441.10	188.12	− 2.34	− 809.74	− 74.25	0.020

Left contralateral = left HV and right hippocampal FC; *left ipsilateral* = left HV and left hippocampal FC; *right contralateral* = right HV and left hippocampal FC; *right ipsilateral* = right HV and right hippocampal FC; *inf* = inferior; *L* = left; *R* = right; *SE* = standard error; *CI* = confidence interval; *LL* = lower level; *UL* = upper level.

*
Significant after correcting for multiple comparisons.